Real-time X-ray diffraction measurement of carbon structure during lithium-ion intercalation

H. Asahina *, M. Kurotaki, A. Yonei, S. Yamaguchi, S. Mori

Tsukuba Research Center, Mitsubishi Chemical Corporation, 8-3-1 Chuo, Ami, Inashiki, Ibaraki 300-03, Japan

Abstract

A coin-type X-ray diffraction (XRD) cell was constructed using synthetic graphite, ethylene carbonate (EC)–diethyl carbonate (DEC)-based electrolyte and lithium metal. Real-time in situ XRD measurements of Li-ion intercalation into graphite were carried out in order to investigate kinetic phenomena during discharge and charge cycles under conditions similar to those of actual coin-type batteries. Intercalation started at 0.55 V versus Li/Li^+. At high doping currents, additional growth of lower stage graphite intercalation compounds (GICs) were observed during open circuit after the cell was discharged to 0 V. In 1 M $LiPF_6$/EC + DEC(1:1), the co-existence region of stage-3 and stage-2 GICs appeared at a very low potential around 0.02 V. Based on these observations, we suggest that an intermediate, which may be reduced solvated lithium ion, is formed on the graphite surface during doping and that the intermediate either intercalates into graphite or reacts with electrolyte solution to form a surface film. © 1997 Elsevier Science S.A.

Keywords: Lithium-ion intercalation; Carbon structure; Graphite, Electrolytes

1. Introduction

Although many studies on Li-ion intercalation into carbon materials have been done by in situ X-ray diffraction (XRD) measurement, experimental conditions very different from the actual battery system have been employed. We devised a special experimental cell made by modifying a conventional coin-type battery cell, in order to investigate the kinetic phenomena during charge and discharge cycles and also to study the influence of the electrolyte system and charging conditions on Li-ion intercalation.

2. Experimental

Synthetic graphite powder (Timcal G&T KS44) was used as the carbon material.

The graphite electrode was made by spreading a slurry of graphite and binder on a 3 μm copper foil using the doctor blade method, so that the XRD pattern could be obtained from the back of the copper foil substrate. A 12.5 mm diameter disk was then stamped out of the sheet. The density of graphite was approximately 7 mg/cm². The cell was constructed by stacking the coin-cell cap, lithium metal foil,
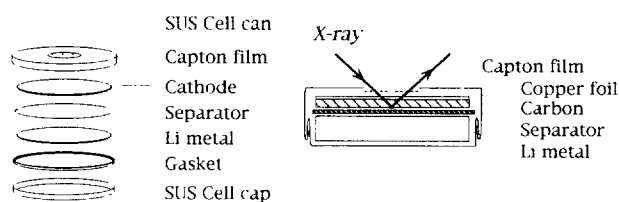

Fig. 1. In situ XRD cell.

separator, graphite electrode (carbon side faces the separator) and the coin-cell top which had a small window made of a capton film (Fig. 1). The coin cell was then hermetically sealed. Ethylene carbonate (EC) and diethyl carbonate (DEC) (Mitsubishi Chemical, battery grade), and $LiClO_4$ and $LiPF_6$ (Tomiyama Chemical, battery grade) were used as received to make 1.5 M $LiClO_4$/EC + DEC(2:8) and 1 M $LiPF_6$/EC + DEC(1:1) electrolyte solutions. XRD data were obtained by using an X-ray diffractometer (JEOL JDX-3500) equipped with a graphite monochromator and with copper target radiated at 30 kV and 300 mA. XRD patterns were taken every 10 min during discharge and charge cycles (in Fig. 3(b), every 70 s). The cell was discharged (intercalation) at a constant current to 0 V versus Li/Li^+, and was kept under open-circuit conditions for 1 h. It was then charged (de-intercalate) to 1.5 V, and was kept under open-circuit conditions for 1 h. The variation of the intercalation behavior was examined: (i) by changing the doping current from 0.2
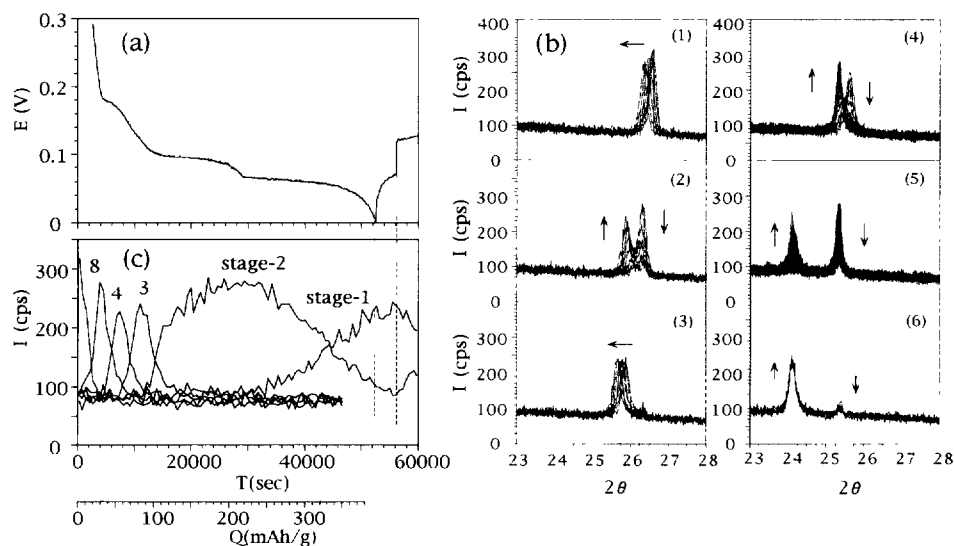
Fig. 2. Potential curve, corresponding variation of XRD patterns and transient phase diagram during Li-ion doping (a) Potential curve vs Li/Li⁺. (b) XRD patterns taken every 10 min during doping. (b-1) 2 to 0.191 V, (b-2) 0.191 to 0.162 V; (b-3) 0.162 to 0.119 V; (b-4) 0.119 to 0.064 V; (b-5) 0.064 to 0.001 V, and (b-6) 0.001 to 0.071 V under open-circuit conditions. (c) Phase diagram taken by plotting peak intensities corresponding to stage-8 (26.22°), stage-4 (25 89°), stage-3 (25.68°), stage-2 (25.28°) and stage-1 (24.02°) with time. Electrolyte solution· 1.5 M LiClO₄/EC + DEC(2:8), doping current: 0.2 mA.

to 4.0 mA in 1.5 M LiClO₄/EC + DEC(2:8), and (ii) by changing the electrolyte solution to 1.0 M LiPF₆/EC + DEC(1:1).

3. Results and discussion

Fig. 2(a) is a potential curve during Li-ion doping at a current of 0.2 mA in 1.5 M LiClO₄/EC + DEC(2:8). Fig. 2(b) shows a typical variation of XRD patterns. The peaks in Fig. 2(b) were assigned to stage-1, -2, -3, -4, -8 and dilute stage-1 according to the assignment of Ohzuku at al. [1] and Dahn [2]. The formation of staged phases and transition to lower stages during Li-ion doping are clearly seen. For example, the (002) peak (26.56°) of the pristine graphite shifted toward lower angles (Fig. 2(b-1) which shows that dilute stage-1 was formed in this region. The peak shift stopped at 26.22° which is assigned to stage-8. In Fig. 2(b-2) the intensity of the stage-8 peak decreased while that of the stage-4 peak at 25.89° increased, indicating that the phase transition from stage-8 to stage-4 occurred. Then the peak shifted smoothly towards lower angles until 25.68° assigned to stage-3 (Figs. 2(b-3), 2(b-4) and (b-5) shows the formation of stage-2 and stage-1, respectively. Fig. 2(b-6) shows the variation of XRD patterns during open circuit after the cell was discharged to 0 V. The intensity of each peak was plotted against time, and transient phase diagrams were obtained as shown in Fig. 2(c). Fig. 3 shows the initial part of the Li-ion doping. At potentials higher than 0.55 V, there was no shift of the pristine graphite peak. At 0.55 V, peak shift started towards lower angle to form dilute stage-1 as shown in Fig. 3(b). This implies that some electrochemical reaction other than intercalation occurred at potentials higher than 0.55 V. We observed the formation of the inorganic
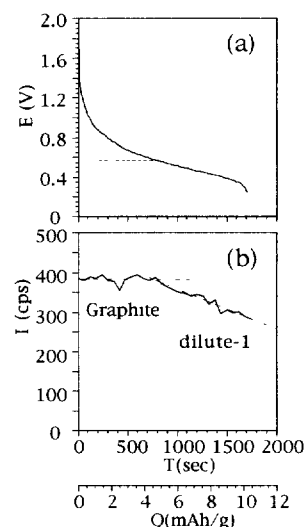

Fig 3 Initial potential curve and corresponding transient phase diagram (a) Potential curve vs. Li/Li⁺. (b) Phase diagram taken by plotting peak intensities corresponding to pristine graphite (26 56°) with time. XRD patterns were taken every 70 s. Conditions were same as that of Fig. 2.

lithium compounds on the graphite surface above 0.55 V, while the organic lithium compounds was formed below 0.55 V [3]. We think that these observations are closely related and that is the clue of initial solid electrolyte interface (SEI) formation mechanism.

Fig. 4 shows the diagrams obtained at 0.6 and 2.0 mA. When the discharge current increased, the potential reached 0 V before stage-1 phase fully grew due to the IR drop. It should be noted that even under open-circuit conditions after the potential reached to 0 V, the fraction of lower stage GICs (i.e. stage-1 in Fig. 4(a), and stage-3 in Fig. 4(b)) increased with time. Similar phenomena were also seen in Fig. 2(c). This phenomena will be discussed later.
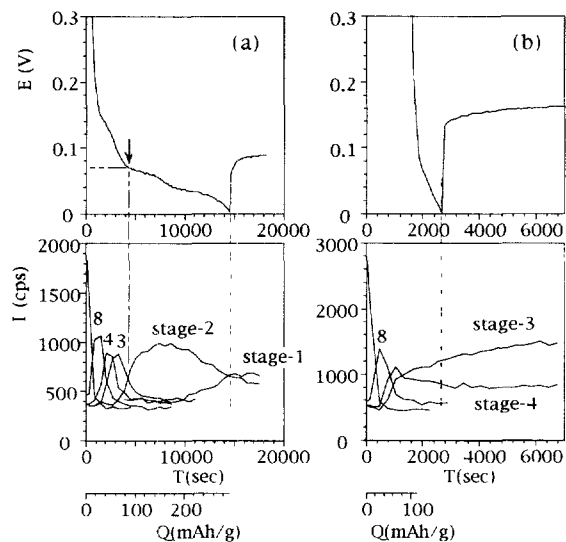
Fig. 4. Variation of potential curves and transient phase diagrams with Li-ion doping rate after several dope/undope cycles: (a) 0.6 mA, and (b) 2.0 mA. The potential at the peak intensities of stage-3 and stage-2 equal to each other is 0.07 V in (a). Electrolyte solution: 1.5 M LiClO$_4$/EC + DEC(2·8)

Fig. 5(a)–(c) shows the potential curves and transient phase diagrams at 0.6 mA dope in the first, second, and third cycles, respectively, in 1 M LiPF$_6$/EC + DEC(1:1). Similar phenomena as above were observed in Fig. 5(a); that is, the fraction of stage-3 and -4 increased, while the fraction of stage-8 decreased under open-circuit conditions. The intercalation efficiency increased with cycle number and also the potential curve changed with cycle number. We interpret this as follows; (i) the diffusion rate of lithium within the graphite is fast enough to match the formation of stage-1 phase at same doping current shown in Fig. 4(a); (ii) so the diffusion rate may not be responsible for the phenomenon that the Li-ion doping terminated far before the formation of stage-1 phase shown in Fig. 5, and (iii) consequently the electrolyte/

graphite interface seems to be more responsible than the graphite interior.

Let us consider the potential curves and GIC-formation diagrams in Fig. 5(b) and (c) with those in Fig. 4(a). Those were obtained at the same current of 0.6 mA. In the first and second cycles in 1 M LiPF$_6$/EC + DEC(1:1) (Fig. 5(a) and (b), respectively), lower stage GICs such as stage-4, stage-3 and stage-2 were formed at potentials lower than in the third cycle. The potential at which the XRD peak intensities of stage-3 and stage-2 became equal (shown by arrow in the figures) was 0.02 V in the second cycle and 0.08 V in the third cycle. This is not due to the IR drop caused by the SEI formed on the surface, because the amount of SEI in the second cycle should not have been more than that in the third cycle. The corresponding potential was mentioned above is 0.07 V in 1.5 M LiClO$_4$/EC + DEC (Fig. 4(a)); this implies that the IR drop caused by SEI was similar to that in the third cycle in 1 M LiPF$_6$/EC + DEC(1:1). However, further doping caused a more rapid decrease in potential in Fig. 5(c) than that in Fig. 4(a). It seems that there existed something to lower the potential at the electrolyte/graphite interface. Now, consider the previously mentioned phenomenon; that is, the fraction of lower stage GICs increased with time under open-circuit conditions. This needs a lithium source somewhere around the interface. According to Inaba et al. [4], when the lithium diffusion in the graphite host is rate determining upon doping, lower stage GICs are formed at the topmost surface while higher stage GICs remain in the interior, and lithium diffuses into the interior under open-circuit conditions. Such a phenomenon would probably occur; however, it is not enough to explain the facts that were observed in this study. Since Figs. 4(a) and 5(a)–(c) were obtained at a constant current of 0.6 mA using the same KS44 graphite powder, the diffusion rate of lithium within the graphite is similar to each other.
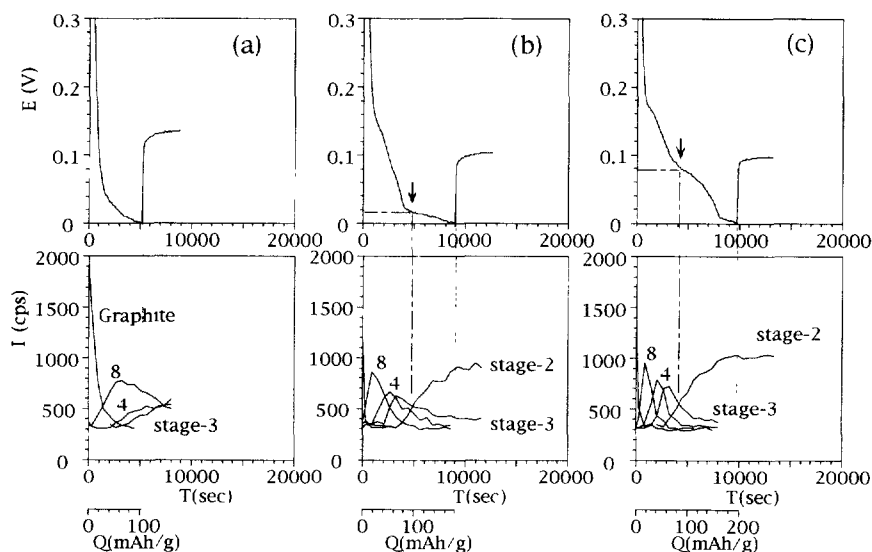

Fig. 5 Variation of potential curves and transient phase diagrams with dope/undope cycle numbers: (a) first dope; (b) second dope, and (c) third dope. The potentials at the peak intensities of stage-3 and stage-2 equal to each other are 0.02 V in (b) and 0.08 V in (c). Electrolyte solution: 1 M LiPF$_6$/EC + DEC(1:1), doping current 0.6 mA.
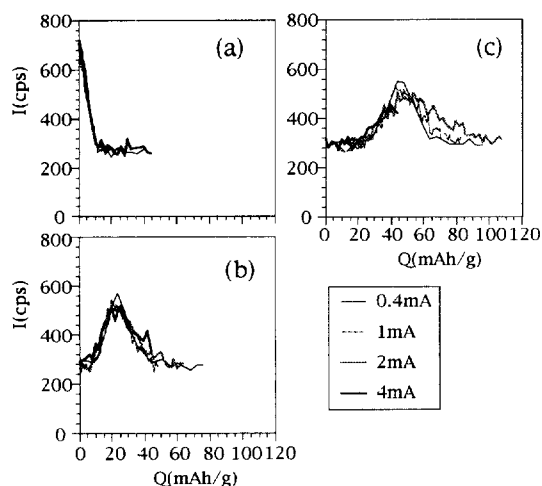
Fig. 6. Comparison of the phase diagram with doping current normalized to the specific charge after several dope/undope cycles: (a) graphite deformation, (b) stage-8, and (c) stage-4. Electrolyte solution· 1 5 M LiClO₄/EC + DEC(2.8).

We propose that an intermediate, which consists of reduced solvated lithium ion, is formed on the graphite surface during doping. Based on our observations: (i) lower stage GIC increased with time under open-circuit conditions. which needs some amount of lithium source, and (ii) the potential in 1 M LiPF₆/ED + DEC(1:1) electrolyte was very low when the GIC structure was similar to that in 1.5 M LiClO₄/ED + DEC(2:8), which needs something to lower the potential on the graphite surface [5,6]. Such an intermediate intercalates into graphite and simultaneously reacts with electrolyte solution to form SEI. Lithium ion is reduced at a constant rate, and when the GIC-formation rate is fast, no intermediate accumulates at the interface. In contrast, when the GIC-formation rate is not so fast, some amount of lithium intermediate accumulates at the interface. This lowers the potential, and the intermediate gradually reacts with solvent to form SEI as seen in Fig. 5. As for the GIC-formation rate, it implies the desolvation rate plus diffusion rate through the electrolyte/graphite interface in the case of Fig. 5(a)–(c) and the lithium-diffusion rate within the graphite in the case of Fig. 4(b).

In order to ascertain the dependence of the diffusion rate upon the GIC structure, the formation rates of dilute-1, stage-8 and stage-4 were measured under several current densities after SEI formation was completed (Fig. 6). The quantity of dilute-1 and stage-8 GICs depended upon only the total amount of charge. However, for the stage-4 formation, the quantity did not merely depend upon the amount of charge but also upon current density. The formation curve of the 0.4 mA dope was sharp, which means the intercalation was probably quantitative while the 2 mA dope needed excess charge to form stage-4 phase, which means that the intercalation was not quantitative. Stage-4 formation was not completed by 4 mA dope, i.e. during the formation the potential reached to 0 V. These observations agree with our intercalation mechanism.

4. Conclusions

By means of real-time XRD measurements of transient GIC formation, the gradual growth of lower stage GICs during open circuit was observed. In 1 M LiPF₆/EC + DEC(1:1) the potential was very low when the GIC structure in the graphite electrode were similar to that in 1.5 M LiClO₄/EC + DEC(2:8). Based on these structural observations and the potential behavior. we propose a mechanism of intercalation that when lithium-reduction rate is faster than lithium-diffusion rate in GIC, an intermediate is accumulated on the graphite surface. This intermediate then intercalates into the graphite and simultaneously reacts with electrolyte to form SEI.

References

[1] T Ohzuku, Y Iwakoshi and K. Sawai, J. Electrochem. Soc., 140 (1993) 2490.
[2] J.R. Dahn, Phys. Rev. B, 44 (1991) 9170.
[3] S. Mori, H. Asahina, H. Suzuki, A. Yonei and K. Yokoto, J Power Sources, to be published.
[4] M. Inaba, H Yoshida, Z. Ogumi, T Abe, Y. Mizutani and M. Asano, J. Electrochem. Soc, 142 (1995) 20.
[5] Z.X. Shu, R.S. McMillan and J.J Murray, J Electrochem. Soc., 140 (1993) 922
[6] M. Arakawa and J-I. Yamaki, J Electroanal. Chem., 219 (1987) 273.